A computed tomography-based radio-clinical model for the prediction of microvascular invasion in gastric cancer

YAHAN TONG[1,2], CAN HU[2,3], XIAOPING CEN[4], HAIYAN CHEN[1], ZHE HAN[1], ZHIYUAN XU[2,3] and LIANG SHI[5]

[1]Department of Radiology, Zhejiang Cancer Hospital, Hangzhou, Zhejiang 310022, P.R. China; [2]Key Laboratory of Prevention, Diagnosis and Therapy of Upper Gastrointestinal Cancer of Zhejiang, Hangzhou, Zhejiang 310022, P.R. China; [3]Department of Gastric Surgery, Zhejiang Cancer Hospital, Hangzhou, Zhejiang 310022, P.R. China; [4]College of Life Sciences, University of Chinese Academy of Sciences, Beijing 100000, P.R. China; [5]Department of Pharmacy, Zhejiang Cancer Hospital, Hangzhou, Zhejiang 310022, P.R. China

Received May 10, 2024; Accepted September 30, 2024

DOI: 10.3892/mco.2024.2794

Abstract. The objective of the present study was to build and validate a radio-clinical model integrating radiological features and clinical characteristics based on information available before surgery for prediction of microvascular invasion (MI) in gastric cancer. The retrospective study included a cohort of 534 patients (n=374 for the training set and n=160 for the test set) who were diagnosed with gastric cancer. All patients underwent contrast-enhanced computed tomography within one month before surgery. The focal area was mapped by ITK-SNAP. Radiomics features were extracted from portal venous phase CT images. Principal component analysis was used to reduce dimensionality, maximum relevance minimum redundancy, and least absolute shrinkage and selection operator to screen features most associated with MI. The radiomics signature was subsequently computed based on the coefficient weight assigned to it. The independent risk factors for MI of gastric cancer were determined using univariate analysis and multivariate logistic regression analysis. Univariate logistic regression analysis was used to assess the association between clinical characteristics and MI status. A radio-clinical model was constructed by employing multi-variable logistic regression analysis, incorporating radiomic features with clinical characteristics. Receiver operating characteristic (ROC) curve analysis, decision curve analysis (DCA) and calibration curves were employed for the analysis and evaluation of the model's performance. The radiomics signature model had moderate recognition ability, with an area under ROC curve (AUC) of 0.77 for the training set and 0.73 for the test set. The radio-clinical model, consisting of rad-score and clinical features, could well discriminate the training set and test set (AUC=0.88 and 0.80, respectively). The calibration curves and DCA further validated the favorable fit and clinical applicability of the radio-clinical model. In conclusion, the radio-clinical model combining the radiomics signature and clinical characteristics may be used to individually predict MI in gastric cancer to aid in the development of a clinical treatment strategy.

Correspondence to: Dr Yahan Tong, Department of Radiology, Zhejiang Cancer Hospital, 1 Banshan East Road, Hangzhou, Zhejiang 310022, P.R. China
E-mail: tongyh2590@zjcc.org.cn

Abbreviations: AI, artificial intelligence; AUC, area under ROC curve; CT, computed tomography; DCA, decision curve analysis; LASSO, least absolute shrinkage and selection operator; OS, overall survival; PCA, principal component analysis; ROC, receiver operating characteristic; SLPP, supervised locality preserving projections

Key words: gastric cancer, radiomics, tomography, X-ray computed, nomogram, microvascular invasion

Introduction

Gastric cancer is currently one of the three deadliest types of cancer in China (1). The accurate identification of tumor aggressiveness and cancer staging are of great significance to achieve appropriate and timely treatment, especially in the preoperative stage, and are also crucial for the development of treatment strategies, diagnosis and prognosis. Microvascular invasion (MI) is closely related to lymph node metastasis and postoperative recurrence of cancer (2,3). The presence of MI is a frequently observed pathological feature in cancer specimens and is widely recognized as a significant prognostic factor for various types of malignancies (4-6). It has been previously shown that MI is associated with poor prognosis of gastric cancer (7). Therefore, understanding the preoperative MI status of patients has clinical significance for individualized treatment selection and prognosis prediction. Unlike conventional macrovascular invasion, MI in gastric cancer is difficult to detect by conventional imaging and can only be detected by postoperative histopathological examination; therefore, preoperative prediction of MI is challenging.

Although traditional imaging methods are indispensable, they do have limitations. Machine learning models can be trained on large datasets to identify subtle abnormalities in images that may not be discernible to the naked eye, thereby providing valuable second opinions and robust evidence for individualized diagnosis and treatment planning (8). With the

introduction of precision medicine, especially the concept of radiomics, the combination of quantitative image analysis and machine-learning methods can be used to extract massive quantitative features from medical images. This facilitates the quantitative analysis of tumors and, further, reveals their heterogeneity, thereby enabling more precise prognosis assessment. It has been identified that the combination of radiomic features and clinical features can answer patients' medical questions in an improved way. Yardımcı *et al* (9) found that computed tomography (CT)-based machine learning has the potential to predict lympho-vascular and perineural invasion in tubular gastric cancer.

A comprehensive model can accurately quantify prognosis at the individual level by combining radiomic features and clinical characteristics, along with other factors. Compared with traditional TNM staging, nomograms established by more clinical characteristics are more effective in predicting the survival of patients with gastric cancer (10,11). For instance, Wang *et al* (11) found that the nomogram established by combining clinical characteristics has a higher value in the preoperative evaluation of the overall survival (OS) of patients with gastric cancer than conventional TNM staging.

Further investigation is warranted to explore the potential of radiomics in predicting the MI status and associated prognosis of gastric cancer. Therefore, in the present study it was aimed to assess the feasibility of establishing a radio-clinical model by integrating radiomic features and clinical risk factors for accurate prediction of MI in patients diagnosed with gastric cancer.

Materials and methods

Patients. The review committee of Zhejiang Cancer Hospital (Hangzhou, China) approved (approval no. IRB-2022-69) the retrospective design of the present study, thereby waiving the requirement for informed consent. A total of 534 patients with a histopathological diagnosis of gastric cancer (including adenocarcinoma and signet ring cell carcinoma) who had undergone radical gastrectomy between April 2008 and October 2012 were identified from the institutional database.

Screening of patients according to the inclusion and exclusion criteria yielded 264 patients who were positive for MI and 270 who were negative for MI. All patients underwent enhanced abdominal CT scan within one month before operation. Inclusion criteria were as follows: i) patients with gastric cancer confirmed by postoperative pathology; ii) abdominal enhanced CT examination was performed within 1 month before the operation; and iii) all surgical specimens were examined for MI status. Exclusion criteria were as follows: i) incomplete clinical or pathological data; ii) received other treatment before surgery; iii) and poor-quality CT image and difficult-to-identify lesions. The cases were randomly divided into a training set (n=374) and a test set (n=160) at a ratio of 7:3. The clinical data of the patients were recorded, including age, sex, tumor location, TNM stage and AJCC stage. The patients were restaged based on the diagnostic criteria outlined in the 8th edition of the American Joint Committee on Cancer Staging Manual. The location of gastric cancer was divided into the cardia, gastric body, gastric antrum and all according to pathology.

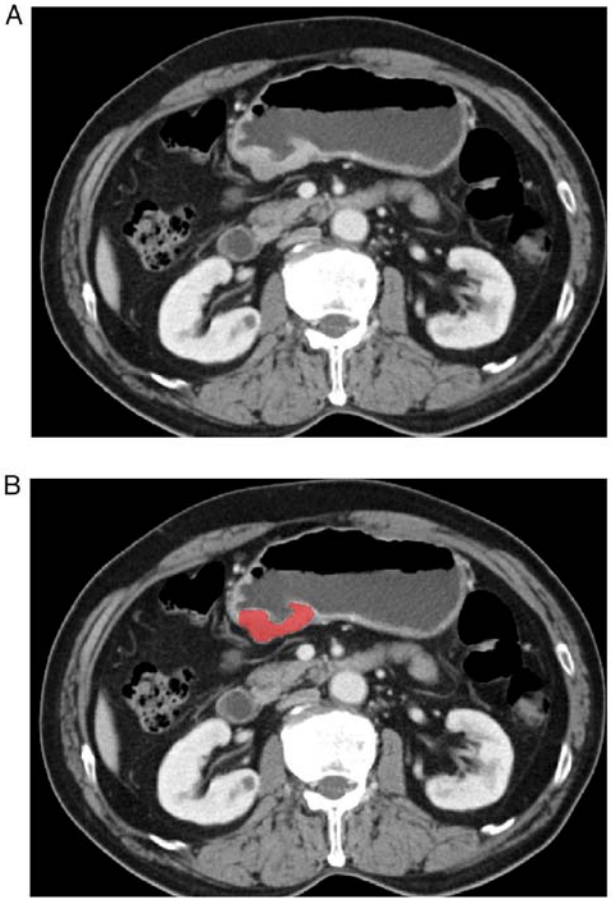

Figure 1. An example of segmentation lesion area in gastric cancer. (A) Localized thick wall of gastric cancer with enhancement is observed on the portal venous phase computed tomography image. (B) Manual segmentation on the same axial slice is depicted with red label.

CT image acquisition. The patients had all undergone enhanced abdominal scanning using multi-slice spiral CT, machine model: GE Optima 680 CT (GE HealthCare), Siemens Somatom definition AS 64, (Siemens Healthineers). The thickness of the reconstructed layer was 5-7 mm. The contrast medium was administered intravenously at a dose of 1.5 ml/kg through the antecubital vein. Contrast-enhanced CT scans were conducted at 30-35 and 50-60 sec after contrast medium injection, respectively.

Histopathology. All patients had received surgical treatment within one month after undergoing contrast-enhanced abdominal CT examination. All surgical specimens had been examined to detect the presence of MI. MI was visible only under light microscopy.

Tumor segmentation. The CT images of patients with gastric cancer were obtained from image storage and communication systems. Digital imaging and communications in medicine format portal phase images were used to delineate the lesions. Region of interest were delineated using ITK-SNAP (version 3.8.0, http://www.itksnap.org). In total, two radiologists with over 5 years of experience in diagnosing gastric diseases meticulously examined each patient's horizontal CT image and accurately delineated the tumor area layer by layer (Fig. 1).

Table I. Clinical and radiological characteristics of patients in training and test sets.

	Training set			Test set		
Characteristic	MI^- (198)	MI^+ (176)	P-value	MI^- (72)	MI^+ (88)	P-value
Age, years			0.614			0.319
mean (SD)	59.4 (9.7)	58.9 (11.1)		58 (10.9)	59.7 (10.7)	
Sex			0.514			0.067
Male	145 (73.2)	135 (76.7)		49 (68.1)	72 (81.8)	
Female	53 (26.8)	41 (23.3)		23 (31.9)	16 (18.2)	
Location			0.063			0.306
Cardia	47 (23.7)	57 (32.4)		18 (25.0)	21 (23.9)	
Body	32 (16.2)	24 (13.6)		10 (13.9)	9 (10.2)	
Antrum	116 (58.6)	87 (49.4)		44 (61.1)	54 (61.4)	
All	3 (1.5)	8 (4.5)		0 (0.0)	4 (4.5)	
T stage			<0.001			0.001
T1	74 (37.4)	8 (4.5)		23 (31.9)	7 (8.0)	
T2	24 (12.1)	23 (13.1)		6 (8.3)	9 (10.2)	
T3	5 (2.5)	3 (1.7)		2 (2.8)	2 (2.3)	
T4	95 (48.0)	142 (80.7)		41 (56.9)	70 (79.5)	
N stage			<0.001			<0.001
N0	112 (56.6)	15 (8.5)		38 (52.8)	15 (17.0)	
N1	39 (19.7)	20 (11.4)		11 (15.3)	10 (11.4)	
N2	31 (15.7)	45 (25.6)		13 (18.1)	22 (25.0)	
N3	16 (8.1)	96 (54.5)		10 (13.9)	41 (46.6)	
AJCC stage			<0.001			<0.001
I	83 (41.9)	6 (3.4)		26 (36.1)	10 (11.4)	
II	47 (23.7)	23 (13.1)		13 (18.1)	10 (11.4)	
III	68 (34.3)	147 (83.5)		33 (45.8)	68 (77.3)	
Rad-sore			<0.001			<0.001
median (IQR)	-0.5 (-0.9, 0.0)	0.3 (-0.2, 0.8)		-0.6 (-1.0, -0.2)	0.1 (-0.4, 0.5)	

MI, microvascular invasion; AJCC, American Joint Committee on Cancer; IQR, interquartile range.

Observer 1 delineated the lesions of all patients with gastric cancer, and Observer 2 checked the accuracy of tumor delineation. If lesion segmentation was inconsistent between the two radiologists, a consensus was reached after consultation.

Radiomics feature extraction and selection. In the present study, PyRadiomics (version 3.0.1) was used, an open-source library, to extract features. After extracting radiomic features based on the original image dataset, feature data of samples in the original feature set were first analyzed using the principal component analysis (PCA) method to ensure that they were uncorrelated. Then, the maximum relevance minimum redundancy (mRMR) and least absolute shrinkage and selection operator (LASSO) methods were used to select the radiomics features. The radiomic score (rad-score) for each patient was subsequently computed through a linear combination of the selected features, with their respective coefficients in the prediction model being applied as weights.

Construction of a predictive model. First, clinical features were selected by univariate analysis. Multivariate logistic regression analysis, combined with rad-score and clinical risk factors were used to construct a comprehensive prediction model. For easy application, the model was transformed as a visual

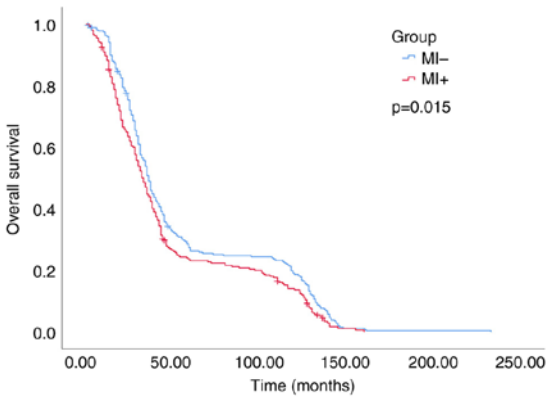

Figure 2. Kaplan-Meier survival analysis of overall survival for all the patients according to microvascular invasion status. P-values were calculated by log-rank test.

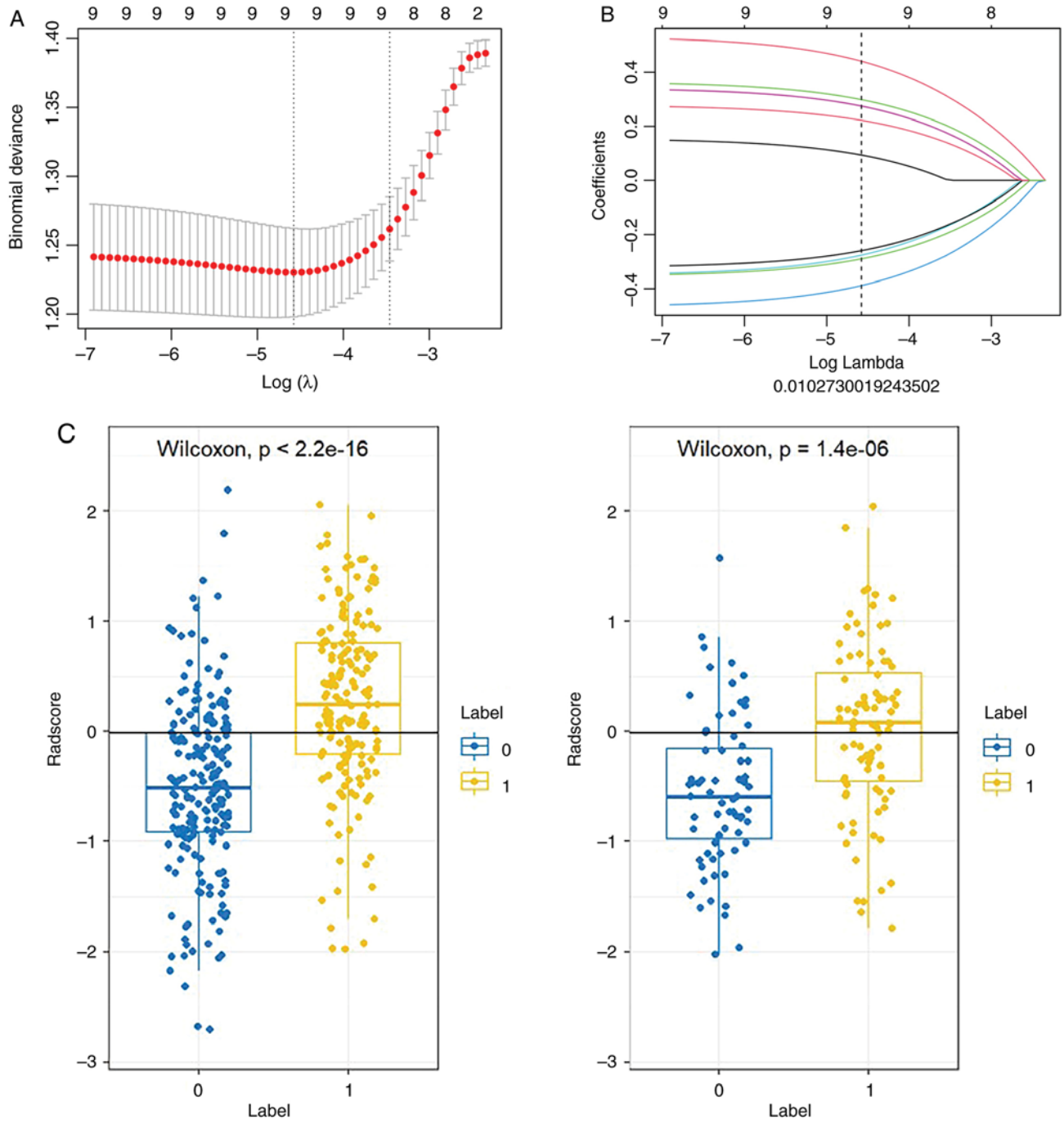

Figure 3. Feature selection with the LASSO logistic regression model and the least absolute shrinkage. (A) The selection of the tuning parameter (λ) in the LASSO model employed a 10-fold cross-validation approach based on minimum criteria. The AUC curve was plotted against the log (λ); (B) The LASSO coefficient profiles depict the coefficients of each feature, with each colored line representing a specific feature. A vertical dotted line is drawn at the selected λ value, indicating where non-zero coefficients were obtained for 9 features. (C) The rad-score of class 0 and class 1 were compared in the training group and the test group, respectively; '0' for no microvascular invasion, '1' for microvascular invasion.

nomogram based on multivariable logistic regression analysis in the training set. Thereafter, the prediction performance of the nomogram was evaluated in the validation set.

Performance of the radiomics nomogram. Receiver operating characteristic (ROC) curve and calibration curve were used to evaluate the predictive efficacy and clinical practical efficacy of the nomogram. Decision curve analysis (DCA) was further employed to evaluate the clinical application value of the model by calculating the net benefits at different threshold probabilities (12). The performance of the model was evaluated by calculating metrics such as the area under the ROC curve (AUC), accuracy, sensitivity, specificity, positive predictive value and negative predictive value.

Statistical analysis. The statistical analysis was conducted using the R software (version 3.4.1; http://www.Rproject.org) and SPSS statistical software (version 26.0; IBM Corp.). The LASSO logistic regression model was employed, and the penalty parameter tuning was performed through 10-fold

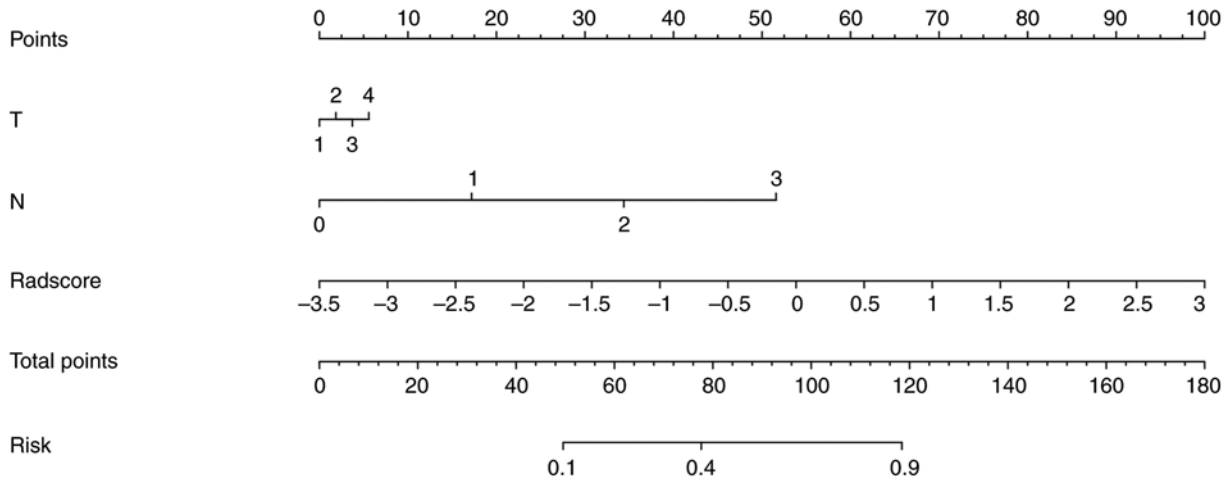

Figure 4. The computed tomography-based radiomics nomogram. The radiomics nomogram was built in the training cohort, with the radiomics signature, T stage and N stage.

cross-validation based on minimum criteria. The Wilcoxon rank-sum test was employed to compare the radscores of class 0 and class 1 in both the training and test groups, respectively. Subsequently, Box-plot were generated using the 'ggplot' package. Continuous variables were represented using mean values and standard deviations, while categorical variables were presented as counts (n) and percentages (%). The independent sample t-test was employed to compare normally distributed continuous data and Mann-Whitney U tests were used for non-normally distributed data. The Chi-square test and Fisher's exact test were utilized to evaluate the distribution of categorical data across groups. Univariate logistic regression analysis was used to evaluate the differences in clinical factors between different groups. The prediction model was constructed by employing multi-variable logistic regression analysis, incorporating rad-score and clinical characteristics. LASSO logistic regression analysis was conducted using the 'glmnet' package. Multivariate logistic regression analysis and calibration plots were performed utilizing the 'rms' package. ROC curves were generated with the 'pROC' package. The 'rmda' package was used to perform the DCA. A range of sensitivity and specificity values were obtained by generating the ROC curve and calculating Youden's index (Youden's index=sensitivity + specificity-1), where the highest value of Youden's index was identified as the optimal cut-off point. The survival probabilities were assessed using Kaplan-Meier survival analysis and the log-rank test. P-values were calculated by log-rank test. $P<0.05$ was considered to indicate a statistically significant difference.

Results

Clinical characteristics. Among 534 patients with gastric cancer, 264 patients had MI and 270 patients did not have MI. The patients were randomly allocated into a training set (n=374) and a test set (n=160) at a ratio of 7:3. In the training and test sets, significantly higher rad-scores were found in the MI group than in the group that was negative for MI ($P<0.01$). Further details are shown in Table I (including sex and age distribution). OS data were also collected from patients and analyzed to compare the difference in survival time between the MI positive group and the negative group. (Fig. 2).

Radiomics features screening and radiomics signature construction. The radiomic features were received from the original CT images of each individual with gastric cancer, resulting in a total of 1,834 features (including shape features, first-order statistics features, texture-based features, higher-order features and features based on model transformation). The feature data of focus were first analyzed by PCA for dimensionality reduction; then, mRMR and LASSO algorithms were employed to identify the optimal subset of features for constructing the radiomics model. A 10-fold cross-validated LASSO logistic regression analysis with a first-rank λ was utilized to select the most relevant radiomic features exhibiting non-zero coefficients (Fig. 3). Finally, 9 radiomic features were selected to establish the radiomics signature; after weighing the selected features, their coefficients were added to calculate the rad-score, and the rad-score of class 0 and class 1 were compared between the training group and the test group, respectively (Fig. 3).

Development of an individualized radiomics nomogram. The clinical variables included sex, age, T stage, N stage, AJCC stage and tumor location. The multivariate logistic regression analysis was conducted based on the results of the univariate analysis, and the odds ratio and 95% confidence interval were subsequently calculated. The predictive model was constructed by integrating multivariate analysis with rad-score and T and N staging, which was further visualized as a radiomic nomogram (Fig. 4). The nomo-score was calculated as follows:

*Nomoscore = (Intercept) * –2.043 + T*0.119 + N * 1.097 + Radscore * 0.982*

Performance of the clinical-radiomics model. The performance results of the three prediction models in the training and test sets are listed in Table II. Radiomics prediction model shows only general prediction ability, as revealed in Fig. 5. The AUC values for the training and test sets were 0.77 and 0.73,

Table II. Predictive performance of the three models.

	AUC (95% CI)	Accuracy	Sensitivity	Specificity	PPV	NPV
Radiomics						
Training set	0.77 (0.72-0.82)	0.709	0.665	0.747	0.701	0.715
Test set	0.73 (0.65-0.81)	0.675	0.580	0.792	0.773	0.606
Clinics						
Training set	0.85 (0.81-0.89)	0.786	0.795	0.778	0.761	0.811
Test set	0.75 (0.68-0.83)	0.706	0.716	0.694	0.741	0.667
Nomogram						
Training set	0.88 (0.85-0.92)	0.807	0.807	0.808	0.789	0.825
Test set	0.80 (0.73-0.86)	0.731	0.792	0.675	0.693	0.778

AUC, area under the curve; CI, confidence interval; PPV, Positive predictive value; NPV, negative predictive value.

respectively. The clinical-radiomics prediction model was constructed by combining clinical factors and rad-score and had better predictive ability for MI status than the two prediction models alone. The AUCs of the training and test sets were 0.88 and 0.80, respectively (Fig. 5). Both calibration curve and DCA indicated that radiomics nomogram has favorable calibration degree and clinical application value (Fig. 5).

Discussion

The treatment of gastric cancer has entered the era of multidisciplinary collaborative comprehensive treatment centered on surgery, and the prognostic differences for the same treatment among patients at the same stage persist due to the inherent heterogeneity of tumors (13,14). Therefore, accurate determination of the risk factors for postoperative recurrence and metastasis of gastric cancer can provide more suitable treatment methods and preventive measures for patients. MI is an important step in tumor diffusion and metastasis (15,16), and MI status is an important independent predictor of clinical factors affecting patients (17,18).

Medical images are morphological representations of tumor tissues and cells that can reflect tumor heterogeneity (19). Images contain considerable information about tumor biological behavior, and radiomics can extract high-dimensional information. The combined analysis of high-dimensional information obtained from images and clinical markers as a stratification tool holds the most potential in assessing a patient's risk; numerous previous studies have also confirmed this view (20). In the present study, the radiomics features of patients were combined with valuable clinical factors to build a model to predict the MI status of patients with gastric cancer to facilitate the formulation of more suitable individualized treatment plans. The utilization of a user-friendly nomogram incorporating radiomics features and T and N stage demonstrate excellent performance in both cohorts. In 2020, Chen *et al* (21) performed a similar study, but the performance of our model was improved compared with that of Chen's. In the aforementioned study, the AUC of the Clinical-Radscore model integrating clinical features and Radscore is 0.856. There may be two reasons to explain this. First, 1,834 features were extracted from the segmentation of the image, while only 180 features were extracted in Chen *et al*'s (21) study. Higher-order features may contain more valuable information. During feature screening, a more advantageous method was applied. High-dimensional features often contain a large amount of irrelevant and redundant information, which can easily lead to overfitting of artificial intelligence (AI) models, that is, poor performance of models on unseen data. In the present study, PCA was performed on the original feature data to ensure they were uncorrelated. Then, the improved supervised locality preserving projections (SLPP) were used to map the data after PCA while preserving the manifold structure of the feature data, making it easier to distinguish. Finally, the dimensionality of the feature space was reduced according to the cumulative contribution of PCA and the eigenvalue of SLPP. The experimental results showed that the PCA could effectively reduce the redundancy of feature data and improve the classification accuracy. After the dimensionality reduction, the mRMR and LASSO were used to select the features. In medical image-based AI research, LASSO and mRMR are the most commonly used feature filtering algorithms (22,23). First, mRMR eliminates redundant and irrelevant features, retaining a subset of 30 features. Subsequently, the optimized feature subset is selected using LASSO to construct the final model. The LASSO algorithm offers two key advantages: First, it avoids overfitting by selecting features based on their univariate association with the outcome; second, it enables the combination of a chosen set of features into a label. In the present study, 9 radiomics features associated with MI were specifically selected to construct radiomics signature to unveil tumor biological attributes that may not be apparent in conventional CT images. Subsequently, the rad-score is calculated by integrating these 9 features weighted by their coefficients. Following this approach, it was aimed to develop a radiomics model for predicting MI in patients with gastric cancer. Our radiomics model demonstrated mediocre discrimination performance with an AUC of 0.77 for the training set and 0.73 for the test set.

Furthermore, although radiomics can answer some of the questions that traditional imaging interpretation cannot, it cannot answer all questions related to clinical decision making.

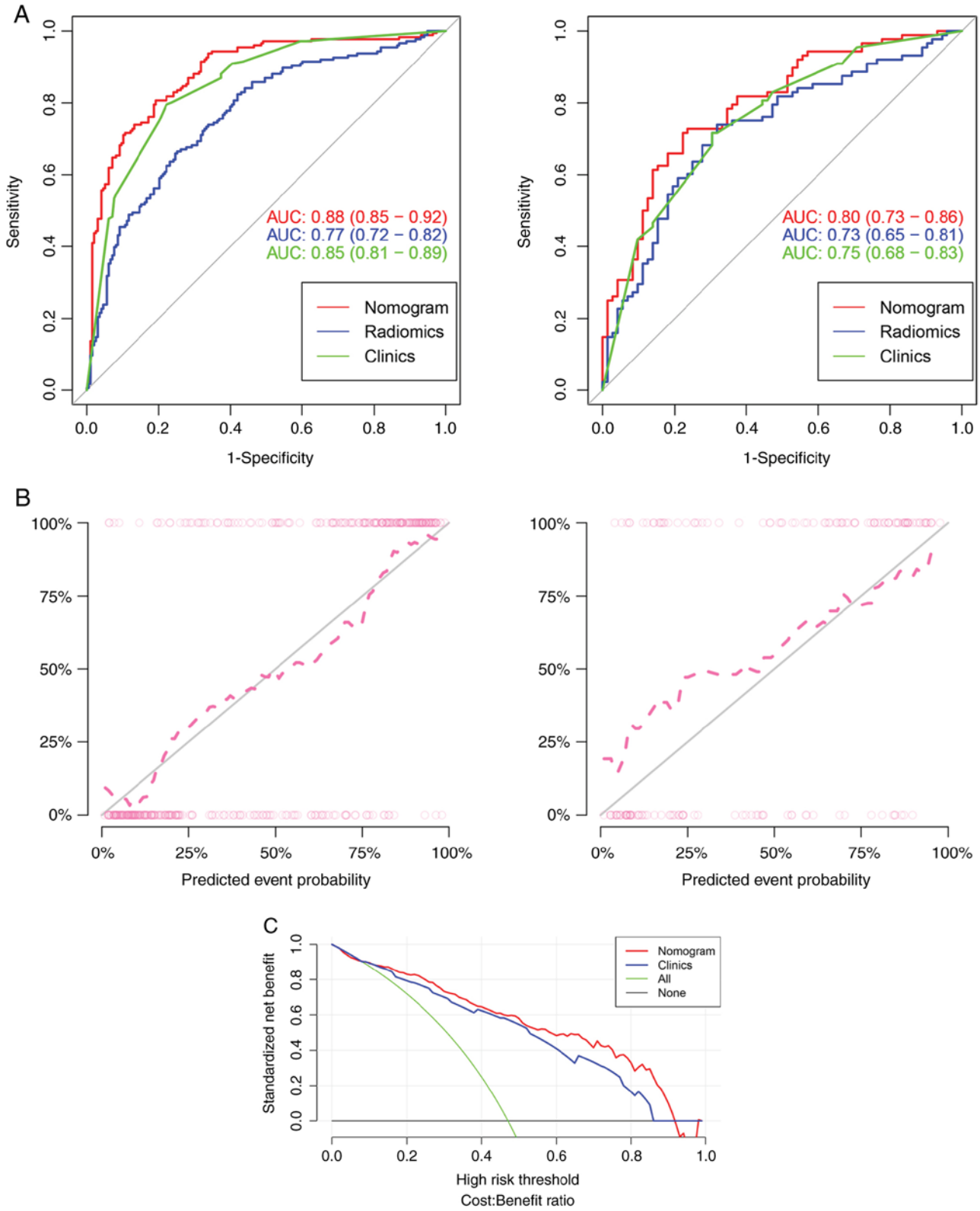

Figure 5. Performance of the radiomics model, clinical model and radio-clinical model. (A) The ROC curves of the three models (radiomics model, clinics model and radio-clinical model) in the training and test sets. (B) Calibration curves of the nomogram in the training set and test set, suggesting that the prediction model is acceptable. (C) Decision curve analysis (DCA) for the radio-clinical model and clinical model. The DCA indicated that more net benefits within the most threshold probabilities were achieved using the radio-clinical model.

The importance of clinical features should not be overlooked in medical problems. Therefore, radiomics was not selected as the only predictor in the present study: Radiomics features were combined with clinically independent risk factors. A previous studies have verified that T stage and lymph node metastasis are independent risk factors for MI (21), and the univariate analysis in the present study reached the same conclusion. However, the two groups did not show any statistically significant differences

in terms of sex, age, or location in univariate analysis. After multivariable analysis, T and N stage were finally included in the nomogram. The combined model achieved an AUC of 0.88 in the training set and 0.80 in the test set, indicating that the clinical-radiomic model exhibited superior predictive performance compared with either model alone. To mitigate the bias resulting from radiologists' erroneous assessments of T and N staging, pathological T stage and N stage were employed for model establishment. In future applications, T stage and N stage judged by CT images may be used instead of postoperative pathological stage, which will be more conducive to the widespread application of the model. The advantage of the present study lies in the inclusion of easily obtainable T and N stage and rad-score in the predictive model, rendering the developed nomogram a reliable and non-invasive tool for preoperative prediction of MI in gastric cancer.

The present study has certain limitations. First, the patient data were retrospectively collected with certain selection biases, highlighting the need for future planned prospective studies. Second, the lack of external validation data necessitates the collection of more multicenter data in future studies to enhance the model's reliability. Finally, numerous previous studies have constructed nomograms to predict clinical events in gastric cancer, and these prediction models can be integrated in the future to provide a more comprehensive and reliable basis for clinicians to formulate individual treatment plans.

In conclusion, the present study demonstrated that the radio-clinical model based on the radiomics signature and T, N stage may be used as a credible and non-invasive modality to predict MI in gastric cancer. This model provided a reliable basis for doctors to choose suitable treatment programs for patients and improve the survival status and prognosis.

Acknowledgements

Not applicable.

Funding

The present study was supported by Medical Health Science and Technology Project of Zhejiang (grant nos. 2021KY583 and 2022KY655) and the Key Laboratory of Prevention, Diagnosis and Therapy of Upper Gastrointestinal Cancer of Zhejiang (grant no. 2022E10021).

Availability of data and materials

The data generated in the present study are not publicly available due to patients' information privacy but may be requested from the corresponding author.

Authors' contributions

YHT completed the initial manuscript and designed the whole study. CH collected patient data and recorded the needed information. ZH and HYC collected imaging data and participated in revising the manuscript. ZYX participated in designing the study. XPC and LS participated in the statistical analysis and provided result interpretation. YHT and CH confirm the authenticity of all the raw data. All authors contributed to the article, and read and approved the final version of the manuscript.

Ethics approval and consent to participate

The present retrospective study was approved (approval no. IRB-2022-69) by the review board of the Medical Ethics Committee of Zhejiang Cancer Hospital (Hangzhou, China). The requirement for informed consent was waived.

Patient consent for publication

Consent for publication was waived for the present study.

Competing interests

The authors declare that they have no competing interests.

References

1. Zheng R, Zhang S, Zeng H, Wang S, Sun K, Chen R, Li L, Wei W and He J: Cancer incidence and mortality in China, 2016. J Natl Cancer Center 2: 1-9, 2022.
2. Wang A, Tan Y, Geng X, Chen X and Wang S: Lymphovascular invasion as a poor prognostic indicator in thoracic esophageal carcinoma: A systematic review and meta-analysis. Dis Esophagus 32, 2019.
3. Hogan J, Chang KH, Duff G, Samaha G, Kelly N, Burton M, Burton E and Coffey JC: Lymphovascular invasion: A comprehensive appraisal in colon and rectal adenocarcinoma. Dis Colon Rectum 58: 547-555, 2015.
4. Sun Q, Liu T, Liu P, Luo J, Zhang N, Lu K, Ju H, Zhu Y, Wu W, Zhang L, *et al*: Perineural and lymphovascular invasion predicts for poor prognosis in locally advanced rectal cancer after neoadjuvant chemoradiotherapy and surgery. J Cancer 10: 2243-2249, 2019.
5. Yuk HD, Jeong CW, Kwak C, Kim HH and Ku JH: Lymphovascular invasion have a similar prognostic value as lymph node involvement in patients undergoing radical cystectomy with urothelial carcinoma. Sci Rep 8: 15928, 2018.
6. Epstein JD, Kozak G, Fong ZV, He J, Javed AA, Joneja U, Jiang W, Ferrone CR, Lillemoe KD, Cameron JL, *et al*: Microscopic lymphovascular invasion is an independent predictor of survival in resected pancreatic ductal adenocarcinoma. J Surg Oncol 116: 658-664, 2017.
7. Fujikawa H, Koumori K, Watanabe H, Kano K, Shimoda Y, Aoyama T, Yamada T, Hiroshi T, Yamamoto N, Cho H, *et al*: The clinical significance of lymphovascular invasion in gastric cancer. In Vivo 34: 1533-1539, 2020.
8. Maniaci A, Fakhry N, Chiesa-Estomba C, Lechien JR and Lavalle S: Synergizing ChatGPT and general AI for enhanced medical diagnostic processes in head and neck imaging. Eur Arch Otorhinolaryngol 281: 3297-3298, 2024.
9. Yardımcı AH, Koçak B, Turan Bektaş C, Sel İ, Yarıkkaya E, Dursun N, Bektaş H, Usul Afşar Ç, Gürsu RU and Kılıçkesmez Ö: Tubular gastric adenocarcinoma: Machine learning-based CT texture analysis for predicting lymphovascular and perineural invasion. Diagn Interv Radiol 26: 515-522, 2020.
10. Hirabayashi S, Kosugi S, Isobe Y, Nashimoto A, Oda I, Hayashi K, Miyashiro I, Tsujitani S, Kodera Y, Seto Y, *et al*: Development and external validation of a nomogram for overall survival after curative resection in serosa-negative, locally advanced gastric cancer. Ann Oncol 25: 1179-1184, 2014.
11. Wang PL, Xiao FT, Gong BC, Liu FN and Xu HM: A nomogram for predicting overall survival of gastric cancer patients with insufficient lymph nodes examined. J Gastrointest Surg 21: 947-956, 2017.
12. Vickers AJ, Cronin AM, Elkin EB and Gonen M: Extensions to decision curve analysis, a novel method for evaluating diagnostic tests, prediction models and molecular markers. BMC Med Inform Decis Mak 8: 53, 2008.
13. Smyth EC, Nilsson M, Grabsch HI, van Grieken NC and Lordick F: Gastric cancer. Lancet 396: 635-648, 2020.

14. Jiang Y, Zhang Q, Hu Y, Li T, Yu J, Zhao L, Ye G, Deng H, Mou T, Cai S, *et al*: ImmunoScore signature: A prognostic and predictive tool in gastric cancer. Ann Surg 267: 504-513, 2018.
15. Zhang CD, Ning FL, Zeng XT and Dai DQ: Lymphovascular invasion as a predictor for lymph node metastasis and a prognostic factor in gastric cancer patients under 70 years of age: A retrospective analysis. Int J Surg 53: 214-220, 2018.
16. Goto A, Nishikawa J, Hideura E, Ogawa R, Nagao M, Sasaki S, Kawasato R, Hashimoto S, Okamoto T, Ogihara H, *et al*: Lymph node metastasis can be determined by just tumor depth and lymphovascular invasion in early gastric cancer patients after endoscopic submucosal dissection. Eur J Gastroenterol Hepatol 29: 1346-1350, 2017.
17. Wu L, Liang Y, Zhang C, Wang X, Ding X, Huang C and Liang H: Prognostic significance of lymphovascular infiltration in overall survival of gastric cancer patients after surgery with curative intent. Chin J Cancer Res 31: 785-796, 2019.
18. Xue L, Chen XL, Lin PP, Xu YW, Zhang WH, Liu K, Chen XZ, Yang K, Zhang B, Chen ZX, *et al*: Impact of capillary invasion on the prognosis of gastric adenocarcinoma patients: A retrospective cohort study. Oncotarget 7: 31215-31225, 2016.
19. Choi SW, Cho HH, Koo H, Cho KR, Nenning KH, Langs G, Furtner J, Baumann B, Woehrer A, Cho HJ, *et al*: Multi-habitat radiomics unravels distinct phenotypic subtypes of glioblastoma with clinical and genomic significance. Cancers (Basel) 12: 1707, 2020.
20. Huang Y, Liu Z, He L, Chen X, Pan D, Ma Z, Liang C, Tian J and Liang C: Radiomics signature: A potential biomarker for the prediction of disease-free survival in early stage (I or II) non-small cell lung cancer. Radiology 281: 947-957, 2016.
21. Chen X, Yang Z, Yang J, Liao Y, Pang P, Fan W and Chen X: Radiomics analysis of contrast-enhanced CT predicts lymphovascular invasion and disease outcome in gastric cancer: a preliminary study. Cancer Imaging 20: 24, 2020.
22. Peng H, Long F and Ding C: Feature selection based on mutual information: criteria of max-dependency, max-relevance, and min-redundancy. IEEE Trans Pattern Anal Mach Intell 27: 1226-1238, 2005.
23. Hepp T, Schmid M, Gefeller O, Waldmann E and Mayr A: Approaches to regularized regression-A comparison between gradient boosting and the Lasso. Methods Inf Med 55: 422-430, 2016.